

A Graphical method for PQ assessment: EDA tools using traditional indices and Higher-order Statistics

P. Remigio-Carmona¹, O. Florencias-Oliveros¹ and J. J. González-de-la-Rosa¹

¹ Research Group PAIDI-TIC-168. Dept. of Automation Engineering, Electronics, Architecture and Computers Networks
University of Cadiz

11202 Algeciras (Spain)

Phone/Fax number: +0034 956 028069, e-mail: paula.remigio@uca.es, olivia.florencias@uca.es,
juanjose.delarosa@uca.es

Abstract. This paper presents a new qualitative method for assessing the power quality (PQ) of electrical systems using both time domain traditional indices and higher-order statistics. The method employs engineering data analysis (EDA) tools to analyse and interpret the PQ data coming from real datasets. Boxplot of each index are considered an essential tool that deserves to be included and studied when an external dataset it is analysed. But this research intends to go a step further, and for this reason a new tool for the spatial visualization of supply quality based on a radar chart is proposed.

Each of its vertices constitutes an index, integrating from 3rd to 6th order statistics with the traditional indicators SNR, SINAD and crest factor. The proposed methodology is applied to the analysis of real available signals and both, boxplot and radar-chart, results are compared and commented. Finally, relationships are established between the altered indicators and the type(s) of event found in the signal.

Key words. Power quality; observational data analysis; visualization tools; higher-order statistics; smart metering; supervised systems

1. Introduction

The increasingly introduction of new distributed energy resources and the incipient dispersion of the users has transformed the modern electrical network drastically, giving rise to the appearance of new and hybrid electrical disturbances. This fact makes clear the growing need to control the Power Quality (PQ) of the electrical network. Power quality refers to the characteristics of an electrical supply that determine its ability to power devices and equipment without interruption or degradation. This includes factors such as voltage, frequency, and harmonic distortion.

Nevertheless, PQ analysis nowadays is a technical topic that remains into the scientific community even when end-users are impacted by. In the smart grid environment, it is increasingly necessary to make information more accessible and understandable for both, utilities and final energy users. For the sake of tackling this challenge, during the last twenty years myriads of new measurement procedures have been developed, all of which have a common axis: the introduction of statistical signal processing to assess PQ [1][2].

For this reason, the incorporation of Exploratory Data Analysis (EDA) becomes crucial. EDA is a method of analysing and summarizing a dataset in order to discover patterns and hidden relationships between data, identify outliers and abnormalities, and generate hypotheses for further investigation under a supervised environment methodology such as an expert system. The goal of EDA is to understand the underlying structure of the data and to uncover any important features or trends that may not be immediately obvious [3].

In the process of following this methodology, many researches have incorporated boxplot as a fundamental tool [4], since this statistical graph allow visualizing whether the distribution of a variable is asymmetric or moving away from the normal distribution, as well as facilitating the comparison of distributions between groups. However, much more information is hidden on indices boxplots. That is why a complementary tool, composed by a holistic analysis of several indicators, is proposed here.

These indicators are displayed in order to introduce additional information that helps the user to extract and compare between traditional and non-traditional indices. Unlike the previously mentioned and already-existing methods, the indicators symbolize the quality of supply and the network status and computes the deviations of the dataset under test from the 50 Hz power supply.

The paper is organized as follows. The next Section 2 contains the methodology followed for signal processing, development and standardization of different tools, and the guidelines followed for the creation of a complementary PQ visualization method. Then, Section 3 shows the process of applying the method to a set of real signals with various disturbances. Finally, conclusions are drawn in Section 4.

2. Materials and methods

Two sets of signals from the same database available in IEEE Dataport have been the basis for the development of the PQ visualization tool [5][6]. In the first group of signals, with durations of approximately one second, real impulsive events are localized. The second group is made

up of real signals of less than 3 seconds duration with sags.

A. Indices

For the signal analysis, two types of indicators have been considered. HOS indices have been used to make a statistical characterisation of the waveform variation caused by several events. In addition, traditional indicators in time domain such as Signal-in-Noise and Distortion (SINAD), SNR and Crest Factor (CF) have also been included [7].

The 3rd order cumulant (skewness, hereinafter represented in the graphs as Sk) and the 4th order cumulant (kurtosis, hereinafter represented in the graphs as K) help to detect transients and the non-symmetry behaviour of the initial and end cycles of events such as sags.

$$Sk = \frac{1}{N} \sum_{j=1}^N \left[\frac{X_j - m}{std} \right]^3 \quad (1)$$

$$K = \frac{1}{N} \sum_{j=1}^N \left[\frac{X_j - m}{std} \right]^4 \quad (2)$$

The 5th and 6th order cumulants (5OC and 6OC, respectively) detect non-gaussian processes and non-linear systems.

$$5OC = E(X - \mu)^5 \quad (3)$$

$$6OC = E(X - \mu)^6 \quad (4)$$

The SINAD and SNR indices help to detect noise processes, providing information about the relative strength of the desired (ideal) signal compared to the noise and distortion present in the system.

$$SINAD = 10 \log \left(\frac{P_s + P_N + P_D}{P_N + P_D} \right) \quad (5)$$

$$SNR = 10 \log \left(\frac{P_S}{P_N} \right) \quad (6)$$

The Crest Factor (CF) quantifies the peakiness of a waveform, so can be used to detect PQ disturbances such as voltage sags, swells and harmonics.

$$CF = \frac{V_{peak}}{V_{rms}} \quad (7)$$

B. Box Plot

This tool under development has been found to well-complement boxplots. An example of this statistical method is shown in figure 1. The segment that divides the box into two parts is the median which facilitates the understanding of whether the distribution of each individual index is symmetric or asymmetric. If the median intersects the box on two unequal sides, there are either positive skewness if the longest part of the box is the upper part of the median, or negative skewness if the longest part is less than the median. One side of the box longer than the other implies that the range is wider, and the data is more spread out.

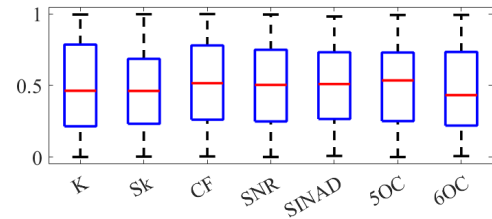


Fig.1.Boxplot's example of indices based on a normal distribution. Notice that, in real analysis each index does not match a normal distribution. That means that maximum values taken here by 1 would reach individual values according to the event magnitude.

For the application in the present research, the obtained boxplots had to be normalized, and had been improved the visualization, due to the great difference in scale between PQ indicators. In this way, each calculated value has been operated with a constant and thus all the values remain between 0 and 1. This allows a more detailed observation of those indices with lower values, not overshadowed by the higher ones. As can also be deduced, in the analysis of ideal signals, the boxplots will show a single line.

C. Radar-chart

Figure 3 shows a multidimensional visualization tool of the PQ. A radar-shaped chart has been considered whose vertices correspond to the aforementioned indicators, selected to provide additional and complementary information between them. Each of these values has had to be normalized and biased so the ideal value of all indices is zero. This state is the shown one in figure 3, result of applying the chart to the ideal signal in figure 2. The maximum values for each indicator, and therefore each vertex, have been defined experimentally from the testing of the radar-chart with synthetic and real signals from IEEE Dataport.

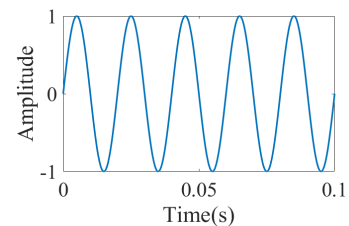


Fig.2.Ideal sinusoidal signal of 50Hz

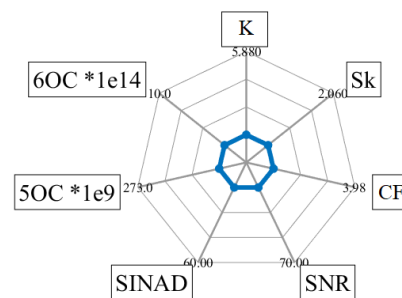


Fig.3.Radar chart from an ideal sinusoidal signal

In the analysis of an ideal 50 Hz signal a perfectly regular polygon is formed on the radar chart. However, in an

event the values will oscillate for each cycle to a greater or lesser extent. These variations will result in a point cloud for each indicator according to the duration of the event, as shown in figure 4. The radar chart helps to detect different states within the disturbance, from the beginning, transition and until the end. The analysis time of the radar chart is adjusted to the duration of the event to be analyzed.

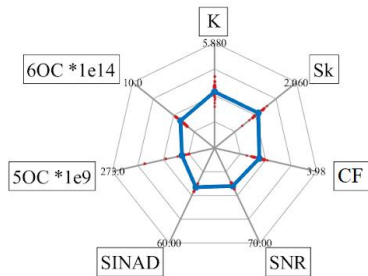


Fig.4.Radar chart's example with point cloud

D. Measurement procedure of EDAS tools using traditional indices and HOS.

Finally, the research follows the procedure here summarized:

- 1) Initially, the signals are extracted from the database. Likewise, the indicators and boxplot are normalized and skewed.
- 2) After this, the calculations are made to obtain a value per cycle of each indicator. With the collected dataset after the complete signal's analysis, the resulting boxplot is obtained. This statistical graph is analyzed and compared firstly with the behavior of synthetic signals and thereafter with the behavior of real signals.
- 3) In the same way, the radar-chart of each cycle is drawn and those that present the greatest alteration of the indicators or different behavior (usually corresponded to the appearance of a disturbance) are compared with the synthetic event if it exists in the database and the chart of a real signal.
- 4) Finally, the characteristic polygonal shapes obtained depending on the type of localized disturbance are considered, since these can vary depending on its nature or the duration of events. Moreover, the area housed in the "limits of the polygon" is obtained as a visual tool to measure overall the waveform deviation changes as a whole and helps to extract conclusions.

3. Results

Initially, the visualization system has been tested with synthetic signals as a calibration, after that, the real-signals database aforementioned has been used. Different real events such as 26 sags and 42 impulsive were available and have been analyzed. These two types of events are used as an example of the empirical method that can be used for a greater number of disturbances. In this document, authors choose to test the feasibility of the proposed visualization tool through those two notable cases of each type of defect are exposed.

A. Boxplot analysis

Following the proposed methodology, in the first instance, the boxplots obtained after the analysis of the indicators in each signal are compared. Figures 5(a) and 5(b) show the boxplot graphed from two impulsive event signals, hereafter, impulsive event 1 (IE1) and impulsive event 2 (IE2), respectively (figure 5 and figures 7 and 8 are the same event). In the same way, figures 6(a) and 6(b) represent the boxplots of the sag 1 (S1) and sag 2 (S2) signals (figure 6 and figures 9 and 10 are the same event).

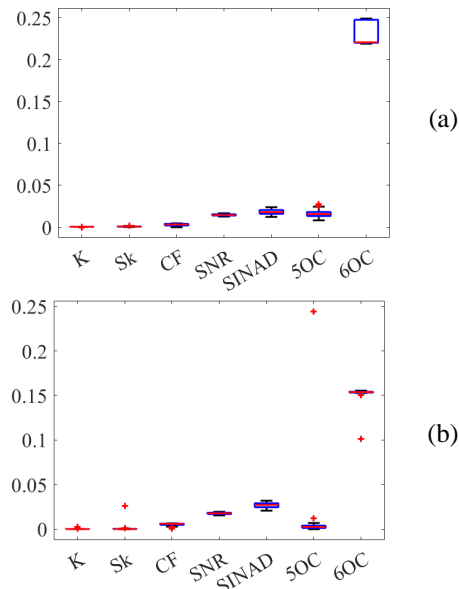


Fig.5. (a) Impulsive event 1 (IE1) signal's boxplot (b) Impulsive event 2 (IE2) signal's boxplot

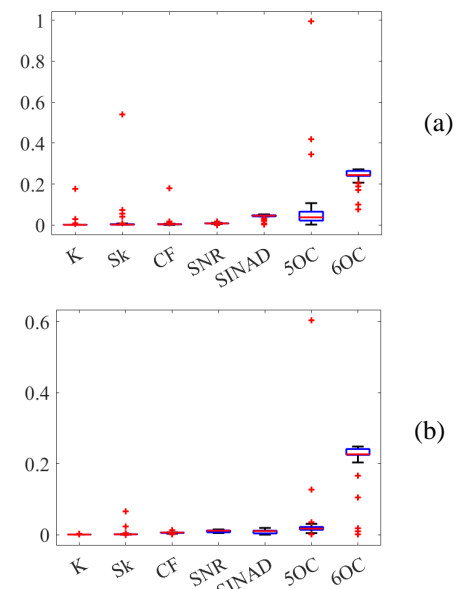


Fig.6. (a) Sag 1 (S1) signal's boxplot (b) Sag 2 (S2) signal's boxplot

Observing both sets of statistical graphs, similarities can be seen between those representatives of the same type of defect. On the one hand, the IE1 and IE2 boxplots present slight blunting in SNR and SINAD, and a more pronounced increase for the 6th order statistic. As a remarkable difference between both graphs, the deviation

of the 6th order cumulant does not remain similar; in IE1 case, it covers a greater range of values with a higher average than in IE2, where this indicator has much more concentrated values with some isolated peaks. The same situation happens with the 5th order cumulant: while for IE1 its value barely stands out, IE2 shows an isolated value much higher than the others. On the other hand, the boxplots from S1 and S2 also present great similarities, both of them maintain levels close to zero except for the 6th order cumulant and some isolated peaks in the higher-order statistics. However, these peak values in S1 are closer to the preset limits for the graph as well as more numerous.

B. Radar-chart analysis

After this analysis, the radar-charts obtained are studied. In the search for a better appreciation of the tool's operation, some of them will be placed in parallel to the display of the signal waveform, indicating which signal cycle each radar belongs to. For IE1, in figure 7, two states stand out: the first one, with a smaller area, is more constant throughout the signal; the second state, marked by the appearance of an impulsive event, shows slightly higher values for SNR and SINAD, which implies that these disturbances are identified as noise.

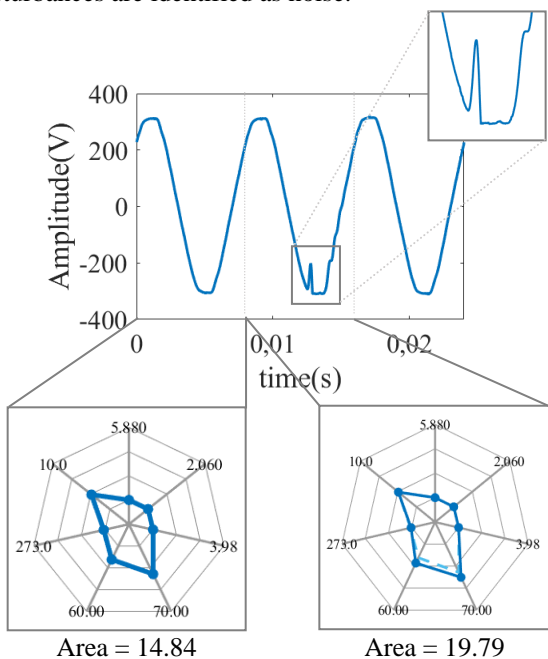


Fig.7. Impulsive event 1 (IE1) signal's radar charts. Clockwise, the values obtained for the chart on the left are: $K=0.006$, $Sk=0.003$, $CF=0.02$, $SNR=31.7$, $SINAD=15.3$, $5OC=5.4$, $6OC=3.2$.

For the chart on the right: $K=0.02$, $Sk=0.003$, $CF=0.03$, $SNR=35.2$, $SINAD=19.8$, $5OC=3.1$, $6OC=3.2$.

In the case of IE2 (figure 8), two states are again considered. The most stationary one preserves a silhouette similar to the obtained ones in IE1. The radar-chart corresponding to the impulse appearance cycle, however, keeps the indicators practically unchanged except for the 5th order cumulant, which increases, indicating an additional non-gaussian feature.

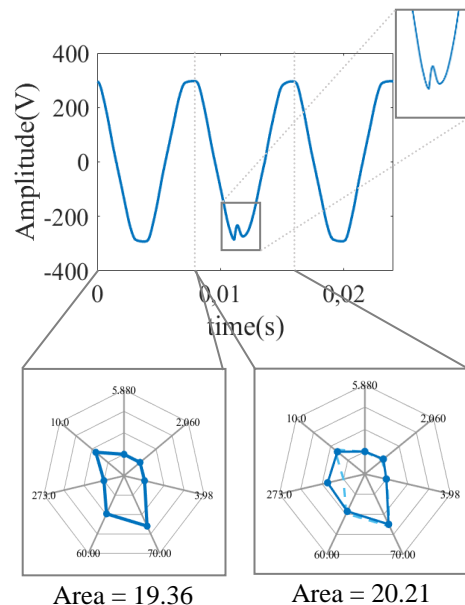


Fig.8. Impulsive event (IE2) signal's radar charts. Clockwise, the values obtained for the chart on the left are: $K=0.001$, $Sk=0.0001$, $CF=0.04$, $SNR=34.0$, $SINAD=24.0$, $5OC=0.2$, $6OC=2.5$.

For the chart on the right: $K=0.04$, $Sk=0.05$, $CF=0.001$, $SNR=35.2$, $SINAD=19.8$, $5OC=67.7$, $6OC=2.0$

Once the results of the signals with impulsive events have been visualized, the sag's signals are observed. In both cases, S1 and S2, three states have been captured: one for the signal before and after the event, another in the transition of appearance of the disturbance and the last one while the sag is taking place.

This evolution for S1 can be seen in figure 9. Between the first and second charts, an increase can be observed in the higher-order statistical indicators, especially in the 5th order cumulant, which indicates an additional non-gaussian feature. One the sag reaches a more stationary state in the third radar, these values drop suddenly being close to ideal values.

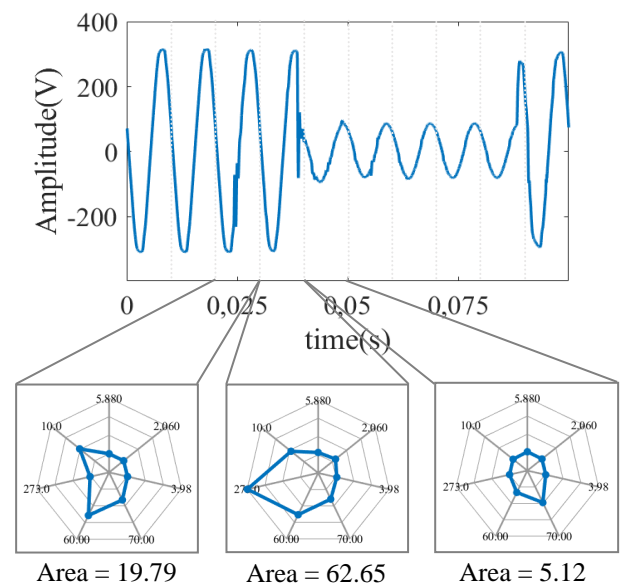


Fig.9. Sag 1 (S1) signal's radar charts. Clockwise, the values obtained for the chart on the left are: $K=0.004$, $Sk=0.01$, $CF=0.03$, $SNR=20.9$, $SINAD=30.4$, $5OC=23.5$, $6OC=3.3$.

For the chart on the middle: $K=0.24$, $Sk=0.15$, $CF=0.06$, $SNR=13.8$, $SINAD=32.8$, $5OC=272.4$, $6OC=3.5$

For the chart on the right: $K=0.08$, $Sk=0.02$, $CF=0.04$, $SNR=21.7$, $SINAD=15.4$, $5OC=0.004$, $6OC=0.001$

Finally, in the three states of S2 there are also changes in the cumulants, this time less significant than in S1, perhaps due to the magnitude of the voltage drop between both cases. Again, the values decay once the disturbance stabilizes, as shown in figure 10.

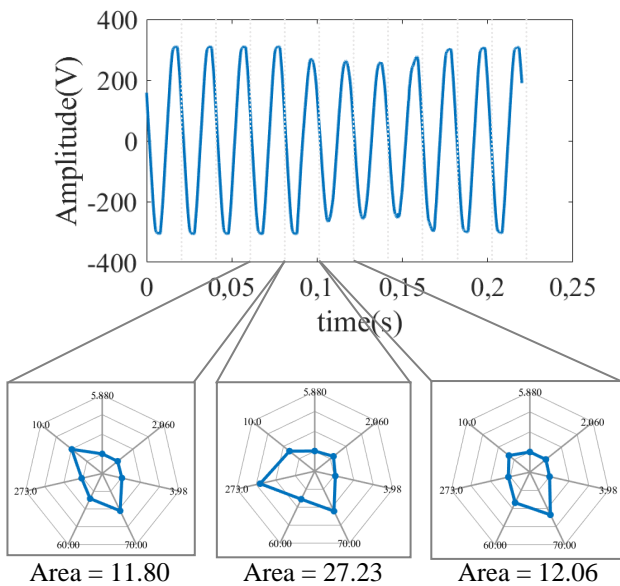


Fig.10. Sag 2 (S2) signal's radar charts. Clockwise, the values obtained for the chart on the left are: $K=0.008$, $Sk=0.004$, $CF=0.04$, $SNR=25.2$, $SINAD=13.7$, $5OC=6.8$, $6OC=3.3$. For the chart on the middle: $K=0.03$, $Sk=0.14$, $CF=0.07$, $SNR=28.4$, $SINAD=10.9$, $5OC=163.9$, $6OC=3.0$. For the chart on the right: $K=0.007$, $Sk=0.01$, $CF=0.005$, $SNR=31.5$, $SINAD=18.2$, $5OC=8.6$, $6OC=1.1$

4. Conclusions

- The radar chart is a tool that provides a comparative overview from the time domain analysis beyond traditional indices. It helps the user to extract and compare traditional and non-traditional indicators. The 5th order cumulant detects transient events, as in IE2 signal, beyond kurtosis, which is not affected.
- When the polygonal area of the signal is scanned cycle by cycle over time, it is observed that initially the polygonal area remains in the same state corresponding to a valid supply. Once a disturbance is reached, a variation of the waveform occurs, and different states are measured.
- Individual indices compute changes, and a hole analysis can be made through the radar chart to extract different patterns (individual indices, polygonal area and patterns) representatives of the network state.
- The length of the window analyzed by the radar is an element that authors are trying to optimize according to the type of event located.
- Authors are working on extend the tool analysis a more robust real signal's database with more types of events analyzed.

Acknowledgement

The authors express their gratitude to the Spanish Ministry of Science and Education for funding the research project PID2019-108953RB-C21, entitled "Strategies for

Aggregated Generation of Photo-Voltaic Plants-Energy and Meteorological Data" (SAGPV-EMOD).

References

[1] Rahul. "Review of Signal Processing Techniques and Machine Learning Algorithms for Power Quality Analysis". *Advanced Theory and Simulations*. 3(10), 2020. doi: 10.1002/adts.202000118.

[2] R. K. Beniwal, M. K. Saini, A. Nayyar, B. Qureshi and A. Aggarwal, "A Critical Analysis of Methodologies for Detection and Classification of Power Quality Events in Smart Grid," in *IEEE Access*, vol. 9, pp. 83507-83534, 2021, doi: 10.1109/ACCESS.2021.3087016.

[3] A. Nasser, D. Hamad, and C. Nasr, "Visualization Methods for Exploratory Data Analysis," Oct. 2006, pp. 1379-1384. doi: 10.1109/ictta.2006.1684582.

[4] S. H. Harbi, G. -C. Seritan, B. -A. Enache and S. -D. Grigorescu, "A Statistical Comparative Study For Detecting Outliers In Electrical Data," 2022 14th International Conference on Electronics, Computers and Artificial Intelligence (ECAI), Ploiesti, Romania, 2022, pp. 1-4, doi: 10.1109/ECAI54874.2022.9847481.

[5] O. Florencias-Oliveros, M. J. Espinosa-Gavira, J. J. González-de-la-Rosa, A. Agüera-Pérez, J. C. Palomares-Salas, J. M. Sierra-Fernández, May 11, 2017, "Real-life Power Quality Transients", *IEEE Dataport*, doi: <https://dx.doi.org/10.21227/H2Q30W>.

[6] O. Florencias-Oliveros, M. J. Espinosa-Gavira, J. J. González de la Rosa, A. Agüera-Pérez, J. C. Palomares-Salas, J. M. Sierra-Fernández, May 11, 2017, "Real-life Power Quality Sags", *IEEE Dataport*, doi: <https://dx.doi.org/10.21227/H2K88D>.

[7] P. Remigio-Carmona, et al. "Potential usages of EDA techniques for PQ analysis in modern instrumentation systems." 2022 IEEE 12th International Workshop on Applied Measurements for Power Systems (AMPS). IEEE, 2022. doi: 10.1109/AMPS55790.2022.9978795.